Earth and Planetary Science Letters 387 (2014) 77–88

Contents lists available at ScienceDirect

Earth and Planetary Science Letters

www.elsevier.com/locate/epsl

Oligocene–Miocene relative (geomagnetic) paleointensity correlated from the equatorial Pacific (IODP Site U1334 and ODP Site 1218) to the South Atlantic (ODP Site 1090)

J.E.T. Channell [a,*], L. Lanci [b]

[a] *Dept. Geological Sciences, University of Florida, Gainesville, FL 32611, USA*
[b] *DiSBeF, University of Urbino, via S. Chiara 27, I-61029 Urbino, Italy*

ARTICLE INFO

Article history:
Received 19 August 2013
Received in revised form 11 November 2013
Accepted 12 November 2013
Available online 5 December 2013
Editor: J. Lynch-Stieglitz

Keywords:
relative paleointensity
Oligocene–Miocene
equatorial Pacific
South Atlantic
IODP Site U1334
ODP Sites 1218 and 1090

ABSTRACT

Late Oligocene to Early Miocene relative paleointensity (RPI) proxies can be correlated from the equatorial Pacific (IODP Site U1334 and ODP Site 1218) to the South Atlantic (ODP Site 1090). Age models are constrained by magnetic polarity stratigraphy through correlation to a common geomagnetic polarity timescale. The RPI records do not contain significant power at specific (orbital) frequencies, and hence there is no significant coherency between RPI proxies and the normalizers used to construct the proxies, although orbital power is present in some normalizers. There is no obvious control on RPI proxies from mean sedimentation rate within polarity chrons, magnetic grain size proxies or magnetic concentration parameters. The salient test is whether the equatorial Pacific records can be correlated one to another, and to the records from the South Atlantic. All records are dominated by RPI minima at polarity reversals, as expected, although the comparison within polarity chrons is compelling enough to conclude that the intensity of the Earth's axial dipole is being recorded. This is supported by the fit of RPI data from Sites U1334 and 1218 after correlation of the two sites using diverse core-scanning data, rather than polarity reversals alone. We do not see a consistent relationship between polarity-chron duration and mean RPI, and no consistent skewness ("saw-tooth" pattern) for RPI within polarity chrons. Stacks of RPI records for 17.5–26.5 Ma include long-term changes in RPI on Myr timescales that are superimposed on RPI minima associated with polarity reversals, and shorter-term variations in RPI with an apparent pacing of ∼50 kyr. The equatorial Pacific to South Atlantic correlations indicate that RPI can be used as a (global) stratigraphic tool in pre-Quaternary sediments with typical pelagic sedimentation rates of a few cm/kyr.

1. Introduction

The equatorial Pacific has been a focus of paleoenvironmental studies of Eocene to Miocene time, due to continuous pelagic sedimentation on long timescales in the high-productivity zone at paleoequator, age control from calcareous/siliceous microfossils/nannofossils, and well-resolved magnetic stratigraphies. The Cenozoic sedimentary record from the equatorial Pacific has been constructed by a series of deep-sea drilling expeditions: Ocean Drilling Program (ODP) Leg 138 (Mayer et al., 1992), followed by ODP Leg 199 (Lyle et al., 2002), and Integrated Ocean Drilling Program (IODP) Expedition 320/321 (Pälike et al., 2010). These expeditions have provided critical information on Eocene to Miocene biotic evolution, changes in calcium compensation depth (CCD), atmospheric CO_2 levels, and astrochronological calibration of the geomagnetic polarity timescale (GPTS) and hence of the geologic timescale (Shackleton et al., 1995; Lyle, 2003; Pälike et al., 2006, 2012). These studies would not have been possible without high-fidelity magnetic polarity stratigraphies that allow largely unambiguous correlation of polarity zones in Cenozoic equatorial Pacific sediments to the GPTS (Schneider, 1995; Lanci et al., 2004, 2005; Pares and Lanci, 2004; Guidry et al., 2012; Channell et al., 2013; Yamamoto et al., 2013; Ohneiser et al., 2013). It has recently been demonstrated that the natural remanent magnetization (NRM) in Cenozoic sediments from the equatorial Pacific is largely carried by sub-micron biogenic (bacterial) magnetite (Yamazaki, 2012; Yamazaki et al., 2013; Channell et al., 2013; Ohneiser et al., 2013). Although biogenic magnetite is ubiquitous in marine surface sediments, and is capable of high-fidelity recording of the ancient geomagnetic field by acquisition of detrital remanent magnetization (DRM), its sub-micron grain size is less resistant to reduction diagenesis than coarser detrital magnetite.

In this paper, we report relative paleointensity (RPI) records for Late Oligocene to Early Miocene from ODP Site 1218 (8.9°N, 224.6°E; ODP Leg 199) and IODP Site U1334 (8.0°N, 228.0°E;

* Corresponding author. Tel.: +352 392 3658; fax: +352 392 9294.
E-mail address: jetc@ufl.edu (J.E.T. Channell).

0012-821X/$ – see front matter
http://dx.doi.org/10.1016/j.epsl.2013.11.028

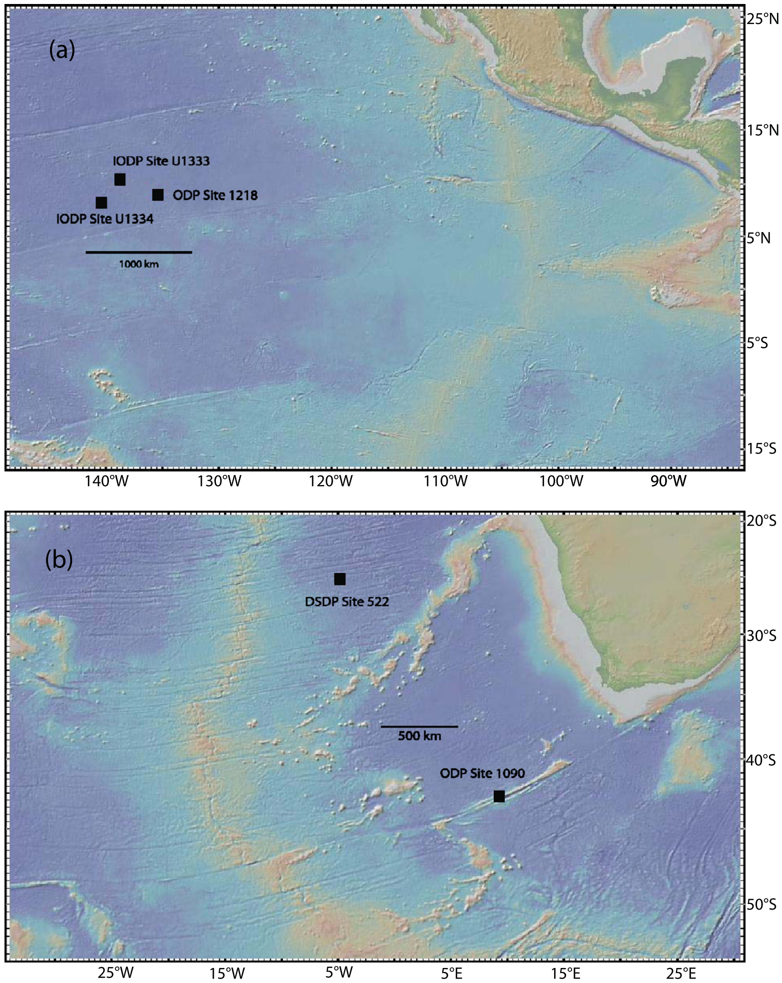

Fig. 1. (a) Location of IODP Sites U1334, U1333 and ODP Site 1218 in the equatorial Pacific, and (b) ODP Site 1090 and DSDP Site 522 in the South Atlantic (from GeoMapApp™).

IODP Exp. 320/321) from the equatorial Pacific, and ODP Site 1090 (42.9°S, 8.9°E; ODP Leg 177) from the South Atlantic (Fig. 1). The RPI records from IODP Site U1334, and ODP Sites 1218 and 1090, are reported here for the first time, although the magnetic polarity stratigraphies were published over 8 years ago in the case of ODP Site 1218 (Lanci et al., 2004, 2005), and over ten years ago in the case of ODP Site 1090 (Channell et al., 2003). New RPI records from equatorial Pacific IODP Exp. 320/321 has made the RPI records from Sites 1218 and 1090 increasingly relevant because potential long-distance correlations provide a means of testing the fidelity of the records. The magnetic polarity stratigraphy from ODP Site 1090 was important not only because it provided an age model for the site, but also because it provided astrochronological calibration of the late Oligocene to early Miocene GPTS (Billups et al., 2004).

Relative paleointensity (RPI) proxies in sedimentary cores are generated by normalizing the intensity of NRM by the intensity of a laboratory-imposed remanence designed to compensate for variations in concentration of remanence-carrying grains down-core (Banerjee and Mellema, 1974; Levi and Banerjee, 1976; King et al., 1983; Tauxe, 1993; Channell et al., 2002). The common normalizers are anhysteretic remanent magnetization (ARM) and/or isothermal remanent magnetization (IRM). The methods are appropriate for pelagic and lacustrine sediments in cases where the sole carrier of magnetic remanence is fine-grained (single domain or pseudo-single domain) magnetite. Although this is commonly the case, marine sediments may incorporate other magnetic minerals as primary components, and changes in magnetic mineralogy commonly occur during reduction diagenesis particularly in parts of the Cenozoic sedimentary sections recovered from the equatorial Pacific (see discussion in Channell et al., 2013).

Numerous RPI records are available for the last ∼1.5 Myrs, mainly from u-channel (continuous) samples of deep-sea cores, and have been used in conjunction with oxygen isotope data as a tool for global correlation (e.g. Channell et al., 2009). Studies of RPI in Oligocene–Early Miocene sediments from Deep Sea Drilling Project (DSDP) Site 522 (South Atlantic, Fig. 1) were carried out over 15 years ago (Hartl et al., 1993; Tauxe and Hartl, 1997; Constable et al., 1998) and until recently there were no comparable RPI records. RPI for an ∼11 Myr interval of Oligocene/Miocene age from DSDP Site 522 was found to be characterized by minima at polarity zone boundaries, lower RPI in the later Oligocene and Miocene when reversal rate was higher (than in the early Oligocene), "weak" correlation of RPI with polarity chron duration, and no persuasive evidence for asymmetric "saw-tooth" profiles (Meynadier et al., 1994) in which abrupt recovery of RPI post-reversal is followed by progressive decrease as the subsequent reversal is approached.

Fifteen years on from the RPI studies at DSDP Site 522, three papers have recently appeared dealing with the long-term Eocene to Miocene RPI records from the equatorial Pacific IODP Sites U1331, U1332, U1333 and U1336 (Yamazaki et al., 2013; Yamamoto et al., 2013; Ohneiser et al., 2013). Ohneiser et al. (2013) considered the RPI record for the middle Miocene from Site U1336 as a "robust" record of geomagnetic paleointensity indicating a gradual decline in field strength between 18.5 Ma and

14.5 Ma, and no discernible link between RPI and either chron duration or polarity state. Yamamoto et al. (2013) found satisfactory RPI correlation among equatorial Pacific sites (U1331, U1332 and U1333) for 30–40 Ma, and considered that RPI records are "generally consistent" between Site U1332 and Site 522 for the 23–33 Ma interval. On the other hand, Yamazaki et al. (2013) considered that the RPI proxies for Eocene–Oligocene sediments from Sites U1331, U1332 and U1333 are contaminated by lithologic factors, and the RPI records are therefore distorted proxies for geomagnetic paleointensity. The contamination is marked by an anti-correlation between RPI and the ratio of anhysteretic remanence to isothermal remanence (ARM/IRM), a magnetite grain-size proxy considered to be a monitor of the proportion of biogenic to detrital magnetite, and by an apparent dependence of RPI on sedimentation rate.

We report RPI records for the 17.5–26.5 Ma interval of the late Oligocene to early Miocene from IODP Site U1334, ODP Site 1218 and ODP Site 1090 (Fig. 1). IODP Site U1334 was occupied during the same expedition (IODP Exp. 320/321) that yielded Sites U1331, U1332, U1333 and U1336, referred to above. The RPI records from IODP Site U1334, ODP Site 1218 and ODP Site 1090 for the 17.5–26.5 Ma interval are compared with the uppermost parts of the RPI records from DSDP Site 522 (Tauxe and Hartl, 1997) and IODP Site U1333 (Guidry et al., 2012; Yamazaki et al., 2013; Yamamoto et al., 2013).

The age models of all sites used in the RPI comparison are based on the magnetic polarity stratigraphies that are published elsewhere: IODP Site U1334 (Channell et al., 2013), ODP Site 1218 (Lanci et al., 2004, 2005), ODP Site 1090 (Channell et al., 2003), IODP Site U1333 (Guidry et al., 2012), DSDP Site 522 (Tauxe and Hartl, 1997). The interpretation of polarity zones in terms of polarity chrons follows these publications, although all interpretations are referred to a common geomagnetic polarity timescale for the Miocene (Lourens et al., 2004) and Oligocene (Ogg and Smith, 2004).

2. Relative paleointensity (RPI) proxies

For ODP Site 1218, ODP Site 1090 and IODP Site U1334, the RPI proxies were measured on u-channel samples and constructed as slopes of NRM demagnetization versus ARM and IRM demagnetization with linear correlation coefficients (r) used to monitor the definition of the slopes (see Channell et al., 2002), using the UPmag software (Xuan and Channell, 2009). The slopes were determined in the 20–60 mT peak demagnetization field interval, in which the peak field increments were 5 mT. IRM was acquired in field of 1 T, and ARM was acquired in 100 mT alternating fields with a 50 μT DC bias field. In the case of Site U1334, an additional normalizer was used: the acquisition of ARM. The ARM acquisition was carried out in increasing alternating fields up to 100 mT, using the same increments used for remanence demagnetization. In this case, the RPI proxy is the absolute value of the slope of NRM demagnetization versus ARM acquisition (see Channell et al., 2008).

For discussion of lithology and magnetic properties at ODP Sites 1090, 1218 and IODP Site U1334, as well as u-channel sampling and measurement procedures, the reader is referred to the papers that give accounts of the magnetic polarity stratigraphy (Channell et al., 2003; Lanci et al., 2004, 2005; Channell et al., 2013). At all three sites, the magnetic properties are dominated by magnetite that has been shown to be partially biogenic (bacterial) at Site U1334 (Channell et al., 2013), and other equatorial Pacific sites (Yamazaki et al., 2013; Ohneiser et al., 2013).

The plot of anhysteretic susceptibility (κ_{ARM}) versus volume susceptibility (κ) can be used to assess magnetite grain size

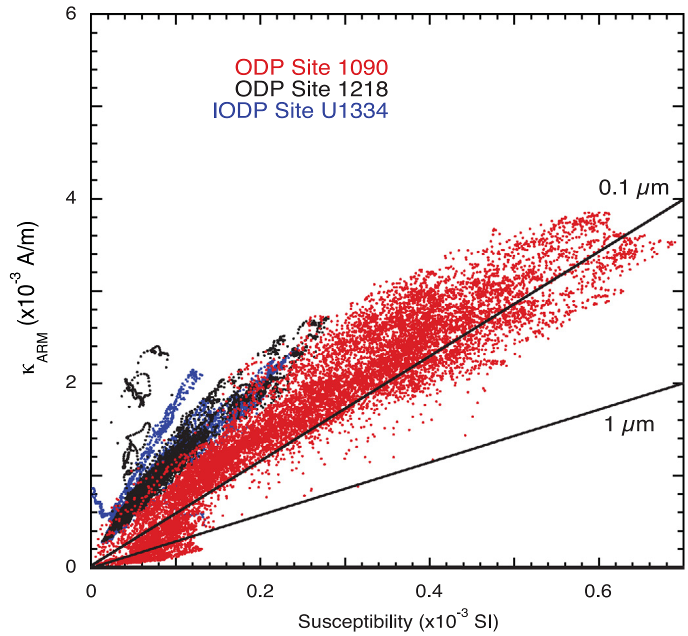

Fig. 2. Anhysteretic susceptibility (κ_{ARM}) after 20 mT peak field demagnetization plotted against susceptibility (κ) for ODP Sites 1090 (red) and 1218 (black), and IODP Site U1334 (blue), with the lines corresponding to the magnetite grain size calibration from King et al. (1983). (For interpretation of the references to color in this figure legend, the reader is referred to the web version of this article.)

(King et al., 1983) where the slopes correspond to a measure of the "mean" magnetite grain size and the distance from the origin corresponds to magnetite concentration. Biogenic (bacterial) magnetite at Site U1334 is characterized by fine grain-sizes (<0.1 μm) on the κ_{ARM} versus κ plot (Fig. 2), and the close correspondence of data points from ODP Site 1218 and IODP Site U1334 implies that ODP Site 1218 magnetite grains are also biogenic in origin. The distribution for ODP Site 1090 spans a larger range of grain sizes and concentrations (Fig. 2), implying a greater contribution of detrital magnetite.

For Site U1334, we plot the three RPI proxies: slopes of NRM/ARM, NRM/ARMAQ and NRM/IRM together with the linear correlation coefficients (r) associated with the slopes (Fig. 3). At Site U1334, the slopes of NRM/ARM and NRM/ARMAQ are virtually identical and therefore not distinguishable in Fig. 3. For Site 1090 (Fig. 4) and Site 1218 (Fig. 5), slopes of NRM/ARM and NRM/IRM are plotted together with the r-values associated with the slopes. NRM/ARMAQ was not determined at Sites 1090 and 1218, as ARM acquisition was not included in our laboratory procedure until recently.

The RPI proxies are generally similar to one another for each individual site, and the r-values are close to unity for most measurements. The exception is the 135–155 mcd and 175–180 mcd intervals of Site 1090 (Fig. 4), where the NRM/ARM and NRM/IRM RPI-proxies are different, and magnetic concentration parameters (ARM, IRM and susceptibility) have low values. For 135–155 mcd at Site 1090, the NRM/IRM slopes mimic the concentration parameters (susceptibility, ARM and IRM) whereas the NRM/ARM slopes do not (Fig. 4), leading us to adopt NRM/ARM as the more appropriate RPI proxy.

For the Eocene–Oligocene RPI records from IODP Sites U1331–U1333 and DSDP Site 522, Yamazaki et al. (2013) noted that peaks and troughs in the RPI proxy (NRM/IRM) tend to be inversely correlated to ARM/IRM, a magnetite grain size proxy. Plots of the RPI proxy versus ARM/IRM (Fig. 7 of Yamazaki et al., 2013) indicate that this inverse correlation holds for Site U1331 and U1332 for ARM/IRM values <0.1, but is not obvious for Site U1333 and Site 522. There is a tendency at Sites U1331–U1333, and DSDP

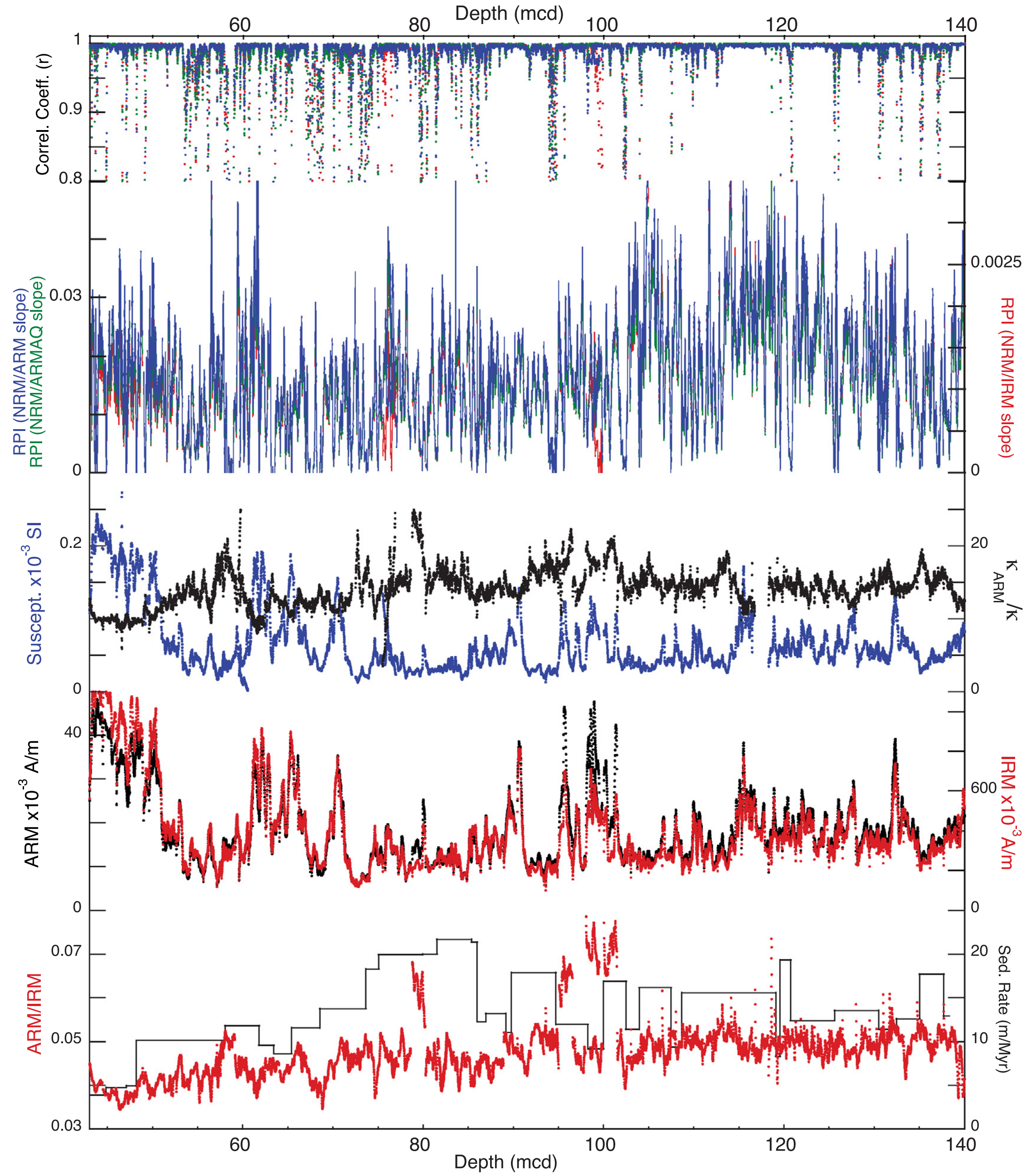

Fig. 3. IODP Site U1334. Relative paleointensity (RPI) proxies from NRM/ARM slopes (blue), NRM/ARMAQ slopes (green) and NRM/IRM slopes (red) determined for the 20–60 mT peak field demagnetization/acquisition interval, with linear correlation coefficients (r) for each slope with the same color coding. ARM and IRM intensities after 20 mT and 35 mT peak field demagnetization, respectively, volume susceptibility (all magnetic concentration parameters), κ_{ARM}/κ and ARM/IRM after 35 mT peak field demagnetization (magnetite grain size parameters) with sedimentation rates based on the magnetic polarity stratigraphy. Depth (mcd) scale from Westerhold et al. (2012). (For interpretation of the references to color in this figure legend, the reader is referred to the web version of this article.)

Site 522, for RPI to increase with increasing sedimentation rate (Fig. 8 of Yamazaki et al., 2013). These observations imply that the RPI proxies at Sites U1331-U1333 are influenced by magnetite grain size (ARM/IRM) and by sedimentation rate. Based on these observations, we investigated how RPI proxies relate to these parameters at Sites U1334, 1218 and 1090.

The relationship between mean RPI within polarity chron and polarity chron duration is represented by a plot of mean RPI and chron duration versus polarity chron sequence (Fig. 6(a)). The relationship is also tested through correlation between chron duration and average stacked RPI (for Sites 1090, 1218 and U1334) within each chron using Kendall's rank correlation test (Fig. 6(b)), which does not require the assumption of a linear relationship between true paleointensity and RPI, as well as Pearson's linear correlation test. The Kendall's $\tau = 0.35$ with a p-value $= 0.0026$, and a correlation coefficient $r = 0.48$ with a p-value of 0.0038, suggest that a moderate degree of correlation is likely, with longer polarity chrons corresponding to higher RPI. However, low values of mean RPI within brief polarity chrons (duration $<$100 kyr) are likely to be affected by low RPI values at reversals, as no attempt was made to exclude RPI at reversals from the estimate of RPI means (Fig. 6(b)). A comparison of mean RPI within polarity chrons with mean sedimentation rate within polarity chrons also shows no obvious relationship (Fig. 6(c)). A plot of NRM/ARM slopes (RPI proxy) versus ARM/IRM indicates that NRM/ARM slopes have a larger range, and ARM/IRM values are lower, for Site 1090 than for Sites U1334 and 1218 (Fig. 6(d)). The differences can be

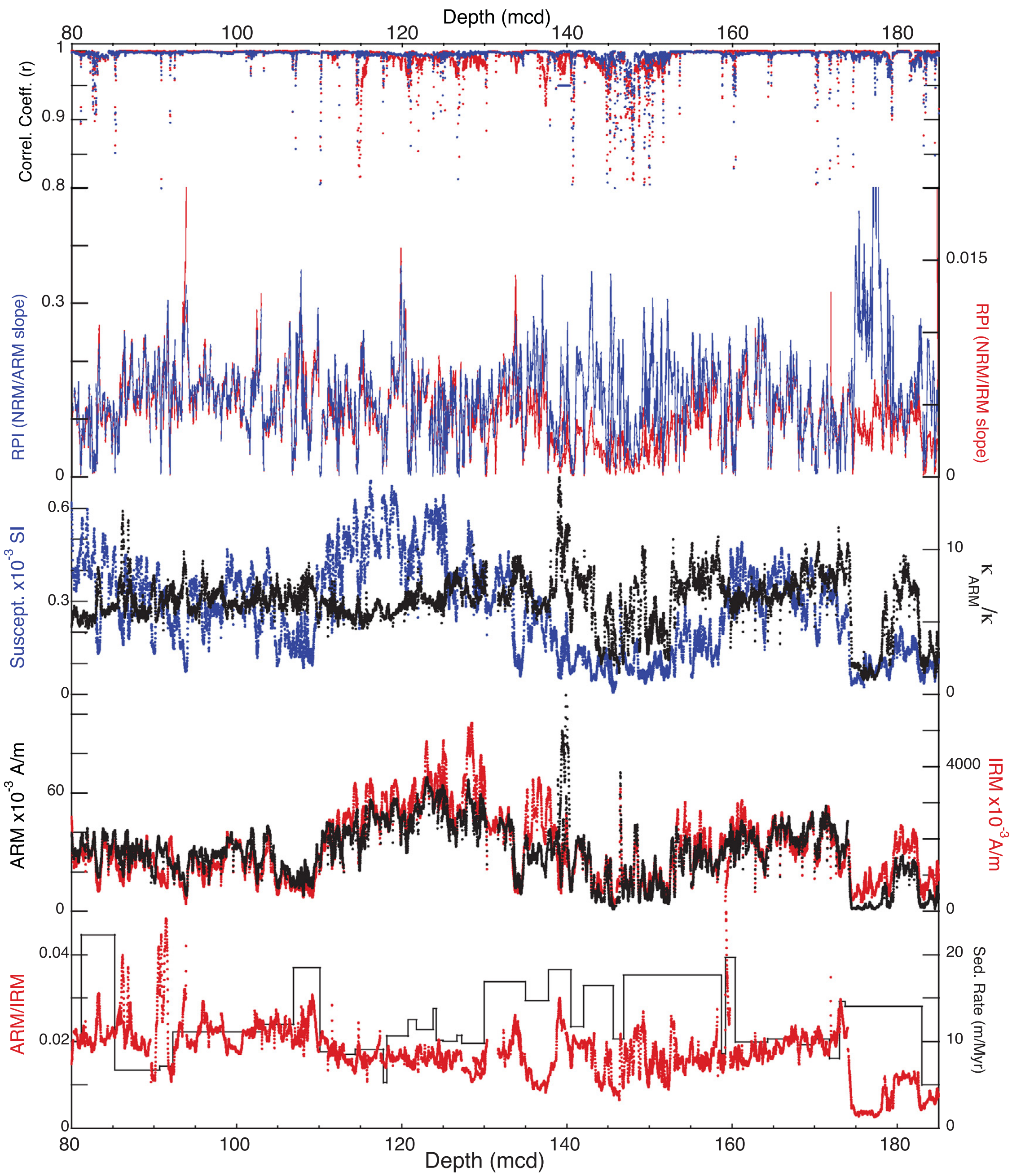

Fig. 4. ODP Site 1090. Relative paleointensity (RPI) proxies from NRM/ARM slopes (blue) and NRM/IRM slopes (red) determined for the 20–60 mT peak field demagnetization interval, with linear correlation coefficients (r) for each slope with the same color coding. ARM and IRM intensities after 20 mT and 35 mT peak field demagnetization, respectively, volume susceptibility (all magnetic concentration parameters), κ_{ARM}/κ and ARM/IRM after 35 mT peak field demagnetization (magnetite grain size parameters), with sedimentation rates based on the magnetic polarity stratigraphy. Depth (mcd) scale from Shipboard Scientific Party (1999). (For interpretation of the references to color in this figure legend, the reader is referred to the web version of this article.)

explained by the importance of fine-grained biogenic magnetite at Site U1334 and 1218, and the increased role of detrital magnetite at Site 1090.

We conclude that RPI proxies (NRM/ARM slopes) at Site U1334 (Fig. 3), Site 1090 (Fig. 4) and Site 1218 (Fig. 5) are not influenced by lithologic variability (magnetite grain size or concentration) and sedimentation rate, at least not in the same way as Sites U1331 and U1332 (Yamazaki et al., 2013). The definitive test for the fidelity of the RPI records is the comparison of the two sites from the equatorial Pacific (Site U1334 and Site 1218) and the site from the South Atlantic (Site 1090). We include in this comparison the parts of the records from Site U1333 and Site 522 that overlap with the interval considered here (17.5–26.5 Ma).

3. Comparison of RPI records (17.5–26.5 Ma)

In order to compare RPI records for 17.5–26.5 Ma spanning the Oligocene–Miocene boundary, we placed all compared RPI records on a common timescale based on the magnetic stratigraphies and their correlation to the 2004 GPTS (Ogg and Smith, 2004; Lourens et al., 2004). Obviously, the synchronization of RPI records can only be expected to be precise at polarity reversals, and as expected, the RPI records placed on a common timescale (Fig. 7) are dominated by RPI minima coincident with polarity reversals. There are, however, similarities in the RPI records that imply that the records are recording a global signal, presumably associated with the Earth's axial dipole field. Changes in RPI are apparent on long (Myr) timescales that are apparently replicated among the

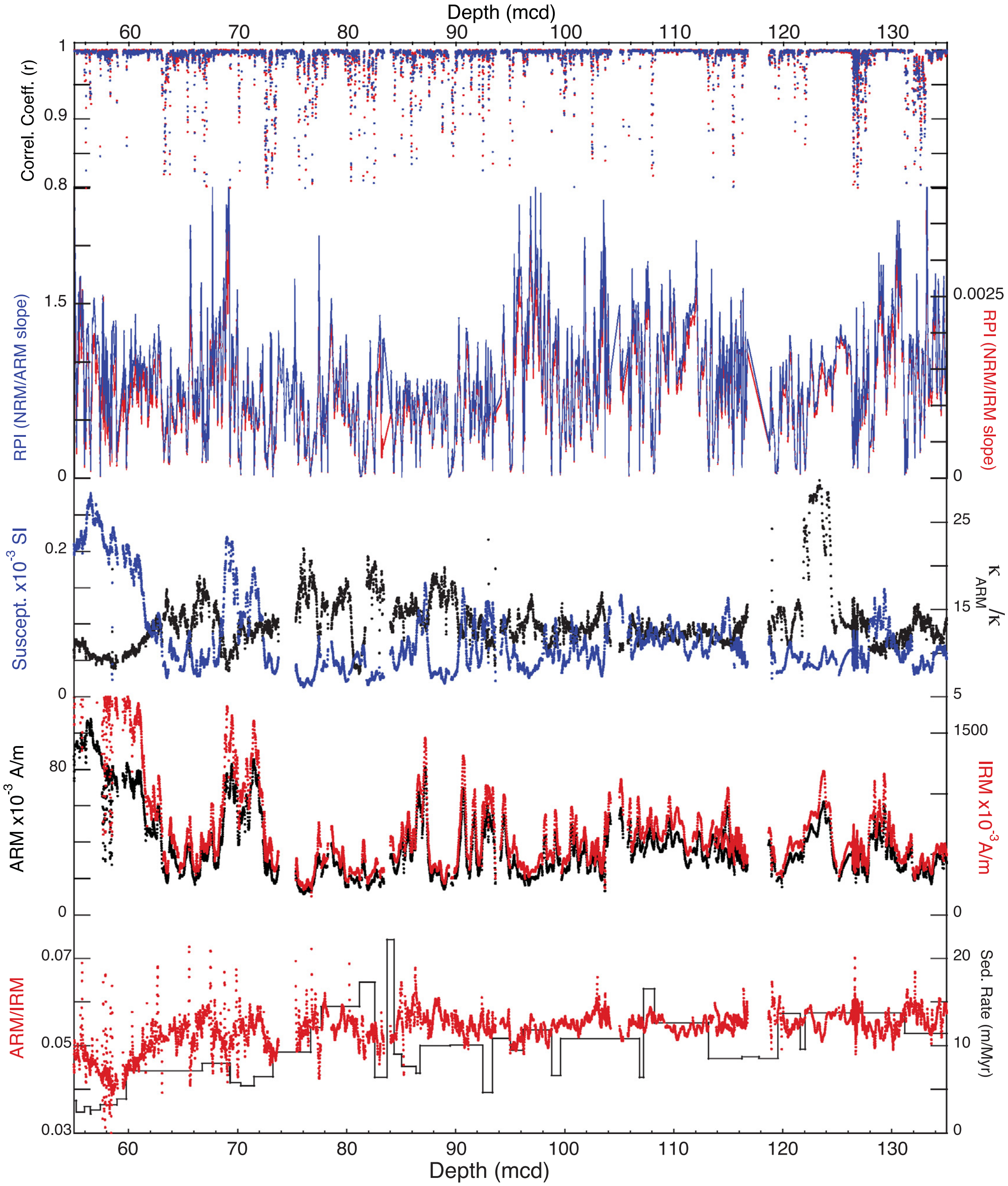

Fig. 5. ODP Site 1218. Relative paleointensity (RPI) proxies from NRM/ARM slopes (blue) and NRM/IRM slopes (red) determined for the 20–60 mT peak field demagnetization interval, with linear correlation coefficients (r) for each slope with the same color coding. ARM and IRM intensities after 20 mT and 35 mT peak field demagnetization, respectively, volume susceptibility (all magnetic concentration parameters), κ_{ARM}/κ and ARM/IRM after 35 mT peak field demagnetization (magnetite grain size parameters), with sedimentation rates based on the magnetic polarity stratigraphy. Depth (mcd) scale from Shipboard Scientific Party (2002). (For interpretation of the references to color in this figure legend, the reader is referred to the web version of this article.)

sites. The comparison of records from the South Atlantic and equatorial Pacific is critical here, because common lithologic variability can probably be ruled out as an explanation for similarity in RPI proxies.

All RPI records represented in Fig. 7 were interpolated to equal (1-kyr) spacing in order to apply methods of spectral analysis, including the MultiTaper method (MTM) (Thomson, 1982; Percival and Walden, 1993; Mann and Park, 1993). Power and coherence spectra are compared with the background red noise estimates at the 99% significance level (Mann and Lees, 1996). For Site U1334 and Site 1218, there is weak but significant power in ARM intensity (one of the RPI normalizers) close to orbital periods of 400, 100 and 41 kyr (Supplemental Fig. 1). There is, however, no significant power in the individual RPI (NRM/ARM) proxies themselves at these periods, and therefore no coherence at the 99% significance level between this RPI proxy and the ARM normalizer (Supplemental Fig. 1).

A stack of the RPI records for the 17.5–26.5 Ma interval (Fig. 8) was constructed by a using a uniform within-record scaling to set all records to a common mean and unit standard-deviation, re-sampling each record by linear interpolation to a common (2 kyr) sample spacing, and then determining the arithmetic mean at 2-kyr intervals and the standard error associated with each mean. The three RPI records from ODP Sites 1090 and 1218, and IODP Site U1334, cover the entire 9-Myr interval. The stacked RPI record derived from these three sites (Fig. 8(a), Supplemental Table 1)

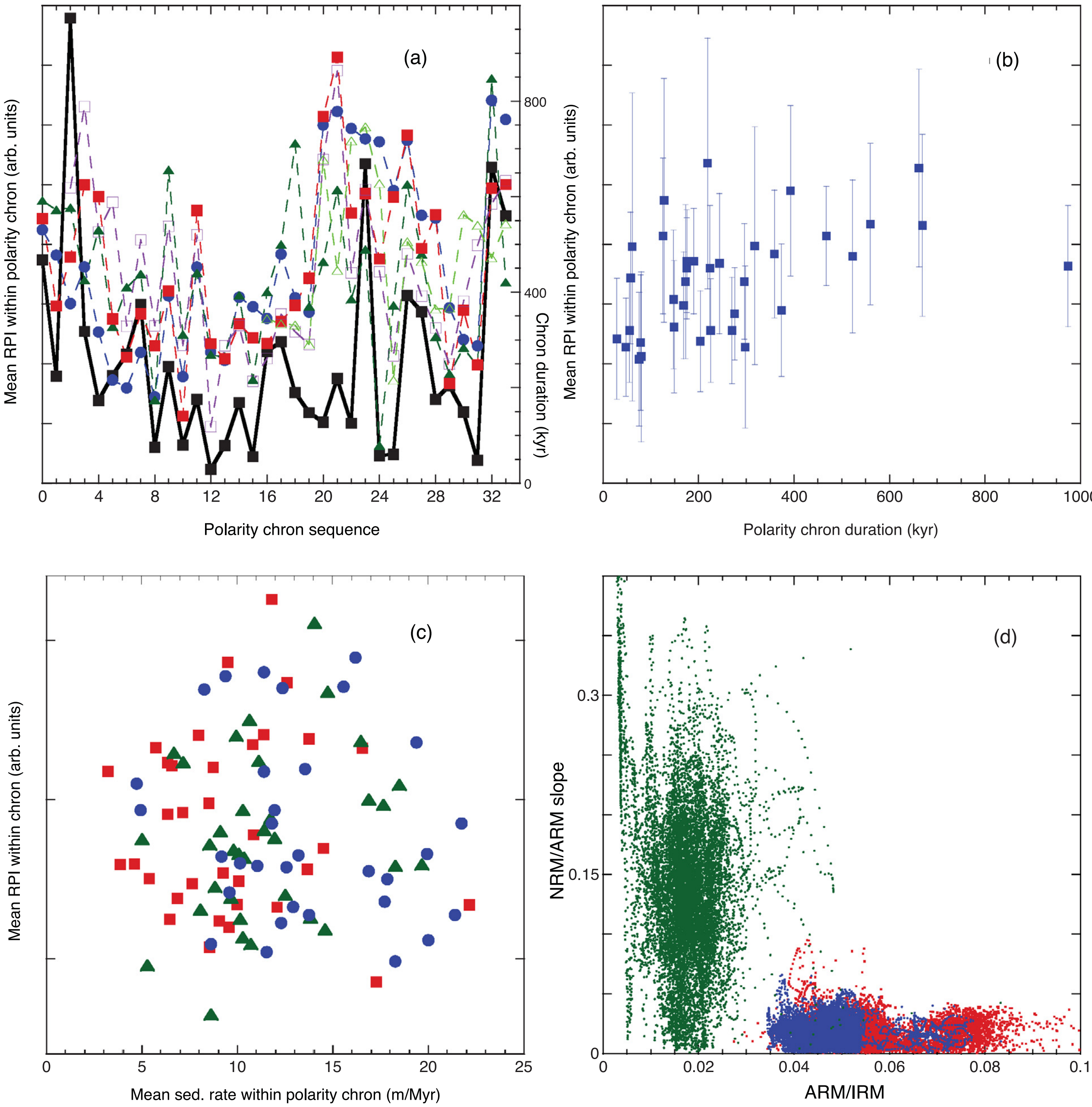

Fig. 6. (a) Mean relative paleointensity (RPI) versus polarity chron sequence (numbered 0–33, young to old) for Site U1334 (closed dark blue circles), Site 1218 (closed red squares), Site 1090 (closed dark green triangles), Site U1333 (open purple squares) and Site 522 (open light green triangles), with chron duration indicated by thick black line with square symbols. (b) Mean relative paleointensity (RPI) versus polarity chron duration for the RPI stack that incorporates data from Sites U1334, 1218 and 1090, with standard deviations. (c) Mean relative paleointensity (RPI) versus mean within-chron sedimentation rate for Site U1334 (dark blue circles), Site 1218 (green triangles), Site 1090 (red squares). (d) The relative paleointensity (RPI) proxy NRM/ARM slope versus ARM/IRM for Site U1334 (dark blue), Site 1218 (red), Site 1090 (dark green). (For interpretation of the references to color in this figure legend, the reader is referred to the web version of this article.)

correlates with each of the 3 individual RPI records with correlation coefficients (r) of 0.80, 0.79 and 0.78 for Sites 1218, 1090 and U1334, respectively. An alternative method to reduce the three RPI records to a single record, using Principal Component Analysis and projecting the data on the 1st eigenvector (i.e., the 1st principal component), was applied to the same three sites and produced a result almost identical (correlation coefficient equals 0.997) to the initial arithmetic stacking (Supplemental Fig. 2).

A fourth RPI record from IODP Site U1333 (Guidry et al., 2012; Yamazaki et al., 2013; Yamamoto et al., 2013) for 18.5–26.5 Ma allows construction of a 4-record stack that can be superimposed on the 3-record stack (Fig. 8b). The RPI record from DSDP Site 522 (Tauxe and Hartl, 1997) for 22–26.5 Ma allows construction of a 5-record stack, superimposed on the 3-record and 4-record stacks in Fig. 8(c). In Fig. 8(a)–(c), the width of the gray error envelope is 2σ, or 2 standard errors.

Using shipboard susceptibility, gamma-ray attenuation (GRA) density, and magnetic polarity information, as well as on-shore X-ray fluorescence (XRF) core scanning, Westerhold et al. (2012) reassessed the hole-to-hole correlations at several ODP and IODP equatorial Pacific drill-sites, including Sites 1218 and U1334. These authors provide an optimal correlation of Sites 1218 and U1334 that is likely to be more precise, particularly within polarity zones, than the correlations based on polarity reversals used in our RPI stacks (Fig. 8). The correlation of RPI records for Sites 1218 and U1334, using the Westerhold et al. (2012) common (Site 1218) depth scale, indicates that the correlation of RPI records from these

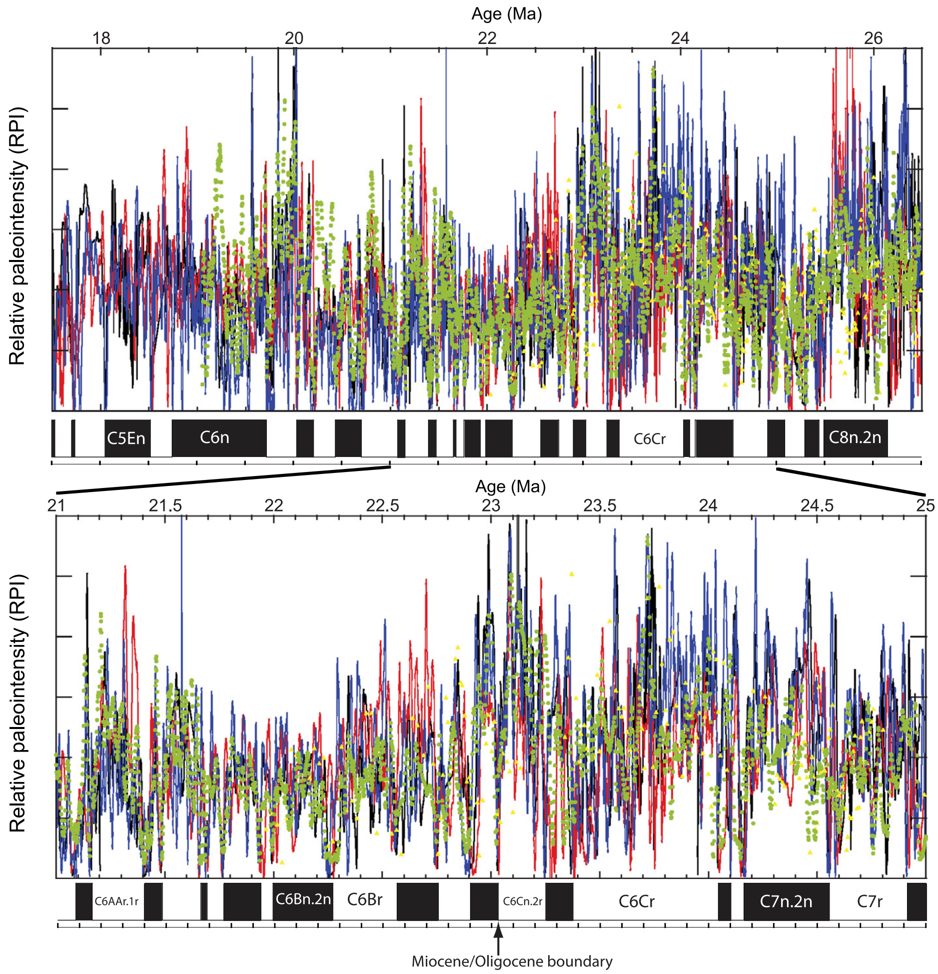

Fig. 7. Relative paleointensity (RPI) proxies (NRM/ARM slope) in the 17.5–26.5 Ma interval (with blow-up of the 21–25 Ma interval), for Site U1334 (blue lines), Site 1218 (black lines), Site 1090 (red lines), Site U1333 (green circular symbols) and Site 522 (yellow triangular symbols) placed on a common age model based on their magnetic stratigraphies and the 2004 geomagnetic polarity timescale where black/white bars represent normal/reverse polarity. (For interpretation of the references to color in this figure legend, the reader is referred to the web version of this article.)

two sites is not only controlled by the position of polarity reversals (Fig. 9). RPI variations within polarity chrons are clearly correlated between the two sites, although the lithologic/color variations observed in the digital image scans (Fig. 9) are also correlated for the two sites separated by 386 km (Fig. 1).

4. Discussion and conclusions

The RPI stack compiled from IODP Site U1334, and ODP Sites 1218 and 1090, where the correlation among sites is based on polarity reversals indicates that the RPI records carry a common signal, not only within the equatorial Pacific, but also from the equatorial Pacific into the South Atlantic (Fig. 8). This correlation can be extended to previously published RPI records from equatorial Pacific IODP Site U1333 (Guidry et al., 2012; Yamazaki et al., 2013; Yamamoto et al., 2013) and South Atlantic DSDP Site 522 (Tauxe and Hartl, 1997). The case for a common RPI signal, at least within the equatorial Pacific, is supported by placing the RPI records from Sites 1218 and U1334 on a common (Site 1218) composite depth based on the core-scanning data (Westerhold et al., 2012). This correlation between these two sites is likely to be more precise than that based on polarity reversals alone, and clearly indicates coeval RPI variations within polarity chrons at the two sites (Fig. 9). There is no clear indication that the mean RPI within polarity chrons is a systematic function of polarity chron duration (Fig. 6(a), (b)) or that RPI varies with mean sedimentation rate within chrons (Fig. 6(c)). For the late Oligocene to early Miocene interval (17.5–26.5 Ma) discussed here, we see no obvious dependence of RPI on ARM/IRM (or other concentration or grain size magnetic parameters) for Sites U1334, 1090 or 1218 (Figs. 3–5, 6(d)).

In Fig. 10, a 1.5-Myr interval of the stack (23.0–24.5 Ma in the latest Oligocene) is compared with the PISO stack for the last 1.5 Myr (Channell et al., 2009), and with a representative record from the last 1.5 Myr from ODP Site 983 (Channell et al., 1997, 2002; Channell and Kleiven, 2000). The PISO stack and the ODP Site 983 record in Fig. 10 are smoothed using 10-point and 20-point running means, respectively, to mimic the lower sedimentation rates for the new Oligocene RPI records (∼1–2 cm/kyr, see Figs. 3–5) compared to the sedimentation rates at ODP Site 983 (∼15 cm/kyr) and for the PISO stack (mean ∼7 cm/kyr). As for the last 1.5 Myr, extreme RPI minima in the Oligocene–Miocene stack are associated with polarity reversals. Other (lesser) RPI minima occur within polarity chrons some of which are known (for the last 1.5 Myr) to be associated with magnetic excursions. A characteristic pacing (roughly 50 kyr) appears similar in both the Quaternary and latest Oligocene RPI segments, irrespective of reversal frequency or polarity state (Fig. 10), and it remains to be seen whether this pacing is an inherent renewal property of the geodynamo. Spectral analysis of RPI proxies indicates marginally

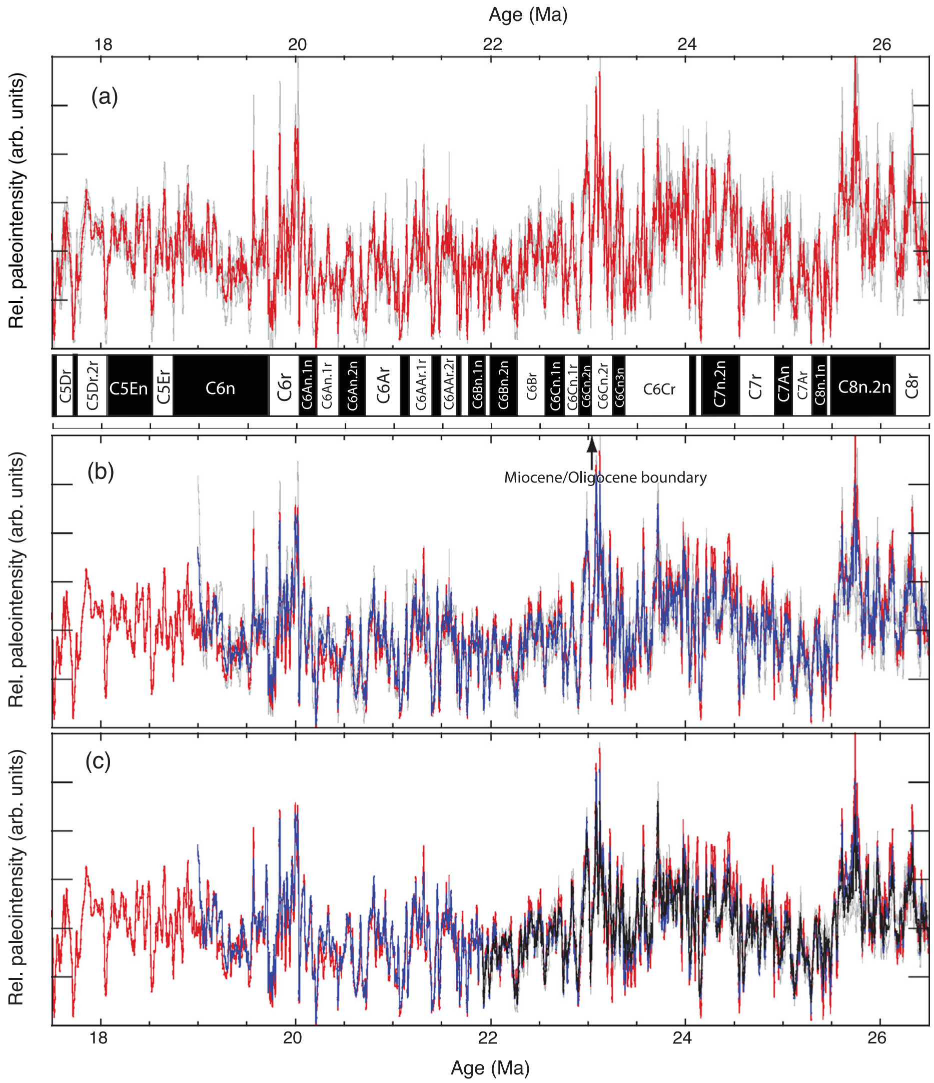

Fig. 8. Arithmetic stack of paleointensity records for the 17.5–26.5 Ma interval. (a) Red: Three-record stack (IODP Site U1334, ODP Sites 1090 and 1218) only. (b) Red: Three-record stack (IODP Site U1334, ODP Sites 1090 and 1218); and in blue: Four-record stack (IODP Site U1334, ODP Sites 1090 and 1218, IODP Site U1333). (c) Red: Three-record stack (IODP Site U1334, ODP Sites 1090 and 1218); in blue: Four-record stack (IODP Site U1334, ODP Sites 1090 and 1218, IODP Site U1333); and in black: Five record stack (IODP Site U1334, ODP Sites 1090 and 1218, IODP Site U1333 and DSDP Site 522). Error bars, represent 2σ (2 times the standard error), are shown in gray for three, four and five record stacks in (a), (b) and (c), respectively. Black (normal) and white (reverse) polarity pattern follows the 2004 geomagnetic polarity timescale. (For interpretation of the references to color in this figure legend, the reader is referred to the web version of this article.)

significant power in the vicinity of frequencies corresponding to periods of ~40–50 kyr (Supplemental Fig. 1).

The long-term (Myr) changes in RPI are present in individual records (Fig. 7), in the resulting stack (Fig. 8), and in the correlation of Sites U1334 and 1218 (Fig. 9) but are not obviously linked to polarity chron duration (Fig. 6(a), (b)). From numerical modeling of the geodynamo (e.g., Glatzmaier et al., 1999; Olson et al., 2010; Courtillot and Olson, 2007), we might expect to see long-term (Myr-scale) changes in RPI related to polarity reversal frequency, with reversal frequency varying with the geometry of core–mantle boundary (CMB) heat flux controlled by global tectonic processes.

RPI, in conjunction with traditional oxygen isotope stratigraphy, has been widely applied as a global stratigraphic tool in the Quaternary (e.g. Channell et al., 2009). The centennial timescales associated with non-axial dipole (NAD) components of the geomagnetic field (e.g., Lhuillier et al., 2011) implies that RPI, when measured in sediments with sedimentation rates less than a few decimeters/kyr, are largely devoid of NAD components are therefore useful for global correlation at millennial or multi-millennial timescales. The results from this study of Oligocene–Miocene sediments from the equatorial Pacific and South Atlantic indicate that the same methods used to resolve Quaternary RPI stratigraphy may be applied to older (Tertiary) sediments to improve the resolution of stratigraphic correlation.

Acknowledgements

Research supported by NSF grant OCE-0960999 (J.C.). We thank Roy Wilkens for providing the digital image scans in Fig. 9, and Toshi Yamazaki for providing relative paleointensity data for IODP Site U1333. We would like to thank the crew and scientists aboard the RV JOIDES Resolution during IODP Exp. 320/321 and ODP Legs 177 and 199, the support staff of ODP and IODP, and the staff of the Bremen Core Repository.

Appendix A. Supplementary material

Supplementary material related to this article can be found online at http://dx.doi.org/10.1016/j.epsl.2013.11.028.

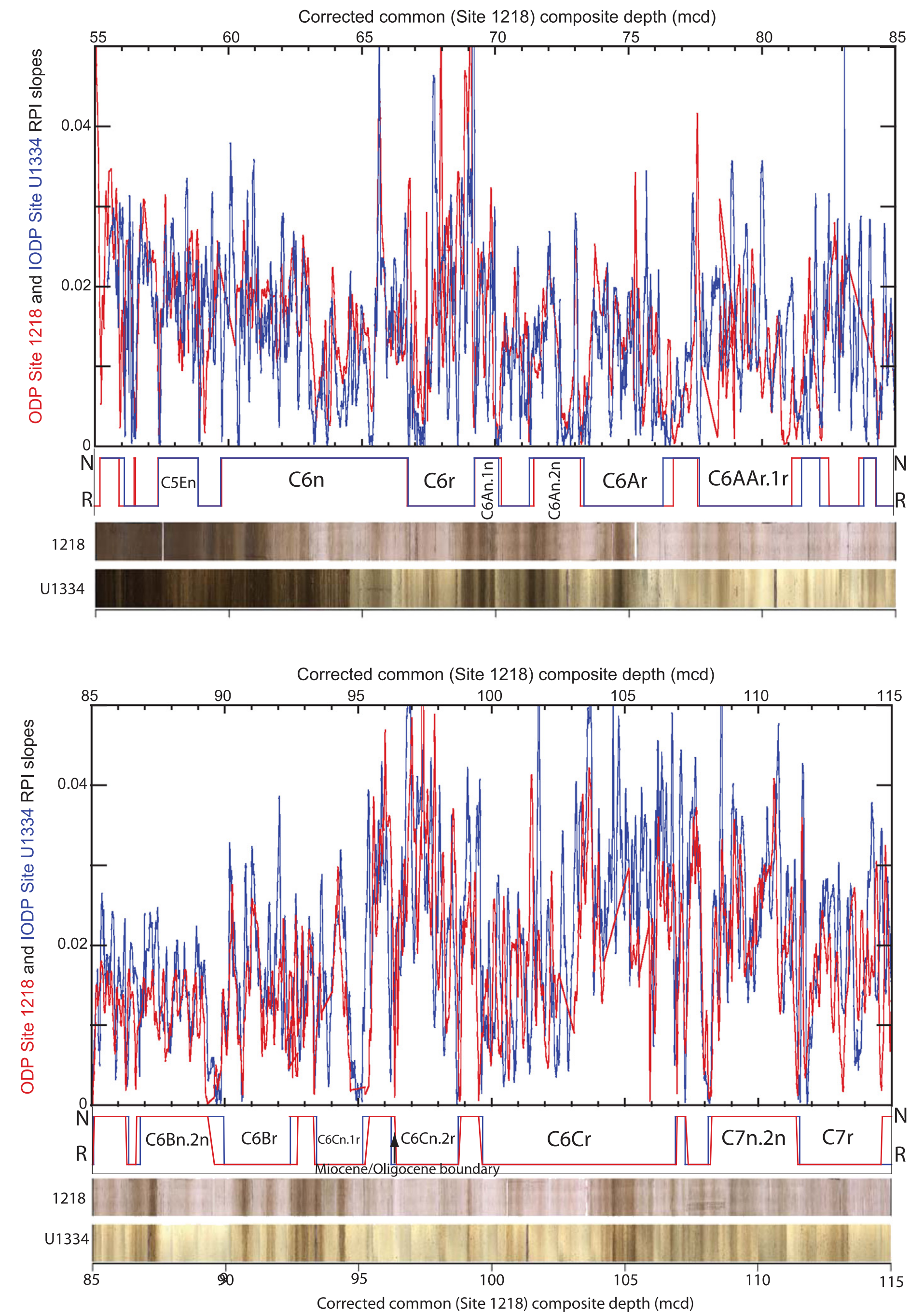

Fig. 9. Correlation of RPI records (NRM/ARM) from IODP Site U1334 (blue) and ODP Site 1218 (red) placed on the common ODP Site 1218 depth scale of Westerhold et al. (2012) where the correlation between the two sites is based on core-scanning data (see text). Normal (N) and reverse (R) polarities are indicated in the same site-dependent color code where slanted lines represent uncertainties in placement of some reversal boundaries. Digital image scans are placed on the same common (ODP Site 1218) depth scale. (For interpretation of the references to color in this figure legend, the reader is referred to the web version of this article.)

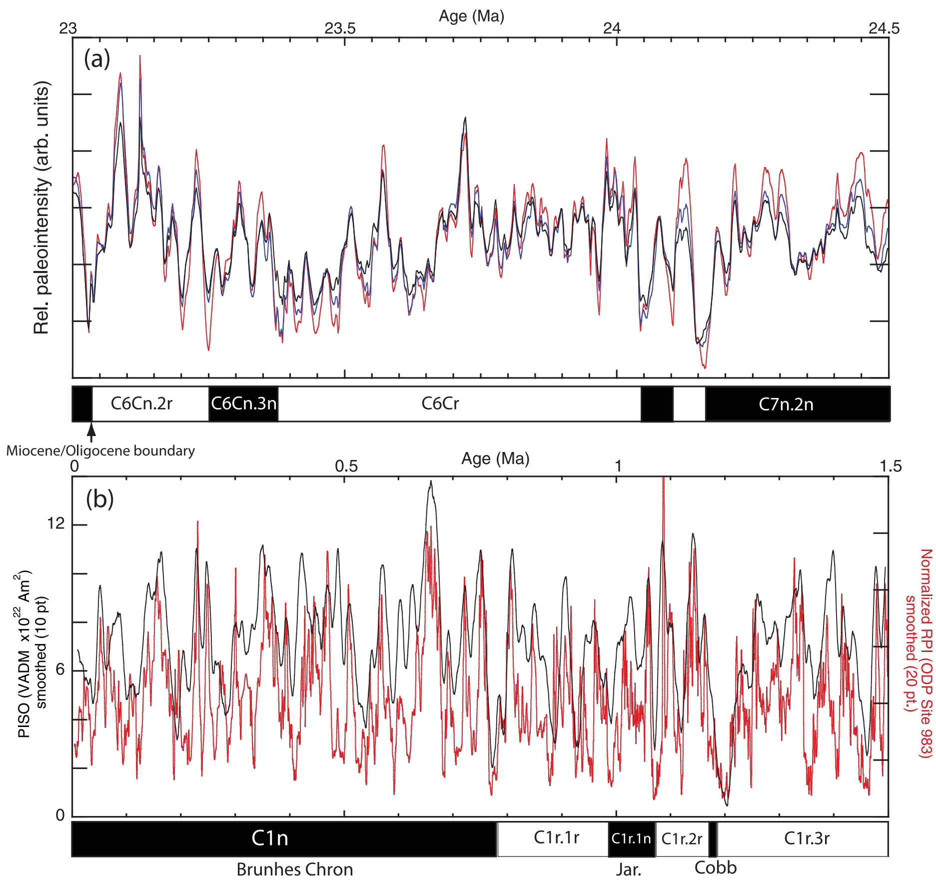

Fig. 10. (a) 1.5-Myr segment of the Late Oligocene part of the stack (23–24.5 Ma) from Fig. 8 where red, blue and black represent the stacks compiled from 3, 4 and 5 record stacks, respectively. Oligocene–Miocene boundary lies at the young end of polarity chron C6Cn.2r. (b) Quaternary relative paleointensity (RPI) PISO stack over the last 1.5 Myr (black), and RPI record for the last 1.5 Myr from ODP Site 983 (red). Black/white bars indicate normal/reverse polarity. (For interpretation of the references to color in this figure legend, the reader is referred to the web version of this article.)

References

Banerjee, S.K., Mellema, J.P., 1974. A new method for the determination of paleointensity from the ARM properties of rocks. Earth Planet. Sci. Lett. 23 (1974), 177–184.

Billups, K., Pälike, H., Channell, J.E.T., Zachos, J.C., Shackleton, N.J., 2004. Astronomic calibration of the late Oligocene through early Miocene geomagnetic polarity time scale. Earth Planet. Sci. Lett. 224, 33–44.

Channell, J.E.T., Kleiven, H.F., 2000. Geomagnetic palaeointensities and astrochronological ages for the Matuyama–Brunhes boundary and the boundaries of the Jaramillo Subchron: palaeomagnetic and oxygen isotope records from ODP Site 983. Philos. Trans. R. Soc. Lond. A 358, 1027–1047.

Channell, J.E.T., Hodell, D.A., Lehman, B., 1997. Relative geomagnetic paleointensity and $\delta^{18}O$ at ODP Site 983 (Gardar Drift, North Atlantic) since 350 ka. Earth Planet. Sci. Lett. 153, 103–118.

Channell, J.E.T., Mazaud, A., Sullivan, P., Turner, S., Raymo, M.E., 2002. Geomagnetic excursions and paleointensities in the 0.9–2.15 Ma interval of the Matuyama Chron at ODP Site 983 and 984 (Iceland Basin). J. Geophys. Res. 107 (B6). http://dx.doi.org/10.1029/2001JB000491.

Channell, J.E.T., Galeotti, S., Martin, E.E., Billups, K., Scher, H., Stoner, J.S., 2003. Eocene to Miocene magnetostratigraphy, biostratigraphy, and chemostratigraphy at ODP Site 1090 (sub-Antarctic South Atlantic). Geol. Soc. Am. Bull. 115, 607–623.

Channell, J.E.T., Hodell, D.A., Xuan, C., Mazaud, A., Stoner, J.S., 2008. Age calibrated relative paleointensity for the last 1.5 Myr at IODP Site U1308 (North Atlantic). Earth Planet. Sci. Lett. 274, 59–71.

Channell, J.E.T., Xuan, C., Hodell, D.A., 2009. Stacking paleointensity and oxygen isotope data for the last 1.5 Myrs (PISO-1500). Earth Planet. Sci. Lett. 283, 14–23.

Channell, J.E.T., Ohneiser, C., Yamamoto, Y., Kesler, M.S., 2013. Oligocene–Miocene magnetic stratigraphy carried by biogenic magnetite at Sites U1334 and U1335 (equatorial Pacific Ocean). Geochem. Geophys. Geosyst. 14, 1–18. http://dx.doi.org/10.1029/2012GC004429.

Constable, C., Tauxe, L., Parker, R.L., 1998. Analysis of 11 Myr of geomagnetic intensity variations. J. Geophys. Res. 103 (B8), 17735–17748.

Courtillot, V., Olson, P., 2007. Mantle plumes link magnetic superchrons to phanerozoic mass depletion events. Earth Planet. Sci. Lett. 260, 495–504.

Glatzmaier, G.A., Coe, R.S., Hongre, L., Roberts, P.H., 1999. The role of the Earth's mantle in controlling the frequency of geomagnetic reversals. Nature 401, 885–890.

Guidry, E.P., Richter, C., Acton, G.D., Channell, J.E.T., Evans, H.F., Ohneiser, C., Yamamoto, Y., Yamazaki, T., 2012. Oligocene–Miocene magnetostratigraphy of deep-sea sediments from the Equatorial Pacific (IODP Site U1333). Geol. Soc. (Lond.) Spec. Publ. 373. http://dx.doi.org/10.1144/SP373.7.

Hartl, P., Tauxe, L., Constable, C., 1993. Early Oligocene geomagnetic field behavior from Deep Sea Drilling Project Site 522. J. Geophys. Res. 98 (B11), 19,649–19,665.

King, J.W., Banerjee, S.K., Marvin, J., 1983. A new rock-magnetic approach to selecting sediments for geomagnetic paleointensity studies: application to paleointensity for the last 4000 years. J. Geophys. Res. 88 (1983), 5911–5921.

Lanci, L., Pares, J.M., Channell, J.E.T., Kent, D.V., 2004. Miocene magnetostratigraphy from Equatorial Pacific sediments (ODP Site 1218, Leg 199). Earth Planet. Sci. Lett. 226, 207–224.

Lanci, L., Pares, J.M., Channell, J.E.T., Kent, D.V., 2005. Oligocene magnetostratigraphy from Equatorial Pacific sediments (ODP Sites 1218 and 1219, Leg 199). Earth Planet. Sci. Lett. 237, 617–634.

Levi, S., Banerjee, S.K., 1976. On the possibility of obtaining relative paleointensities from lake sediments. Earth Planet. Sci. Lett. 29, 219–226.

Lhuillier, F., Fournier, A., Hulot, G., Aubert, J., 2011. The geomagnetic secular-variation timescale in observations and numerical dynamo models. Geophys. Res. Lett. 38, L09306. http://dx.doi.org/10.1029/2011GL047356.

Lourens, L., Hilgen, F.J., Shackleton, N.J., Laskar, J., Wilson, D., 2004. The Neogene period. In: Gradstein, F.M., Ogg, J.G., Smith, A.G. (Eds.), A Geologic Time Scale 2004. Cambridge University Press, pp. 409–440.

Lyle, M., 2003. Neogene carbonate burial in the Pacific Ocean. Paleoceanography 18, 1–21.

Lyle, M.W., Wilson, P.A., Janecek, T.R., et al., 2002. Proc. ODP, Init. Repts., 199 [CD-ROM]. Available from Ocean Drilling Program, Texas A&M University, College Station, TX 77845-9547, USA.

Mann, M.E., Lees, J., 1996. Robust estimation of background noise and signal detection in climatic time series. Clim. Change 33, 409–445.

Mann, M.E., Park, J., 1993. Spatial correlations of interdecadal variation in global surface temperatures. Geophys. Res. Lett. 20, 1055–1058.

Mayer, L., Pisias, N., Janecek, T.R., et al., 1992. Proc. ODP Init. Repts. 138. Ocean Drilling Program, College Station, TX.

Meynadier, L., Valet, J.P., Bassinot, F., Shackleton, N.J., Guyodo, Y., 1994. Asymmetrical saw-tooth pattern of geomagnetic field intensity from equatorial sediments in the Pacific and Indian oceans. Earth Planet. Sci. Lett. 126, 109–127.

Ogg, J.G., Smith, A.G., 2004. The geomagnetic time scale. In: Gradstein, F.M., Ogg, J.G., Smith, A.G. (Eds.), A Geologic Time Scale 2004. Cambridge University Press, pp. 63–86.

Ohneiser, C., Acton, G., Channell, J.E.T., Wilson, G.S., Yamamoto, Y., Yamazaki, T., 2013. A middle Miocene relative paleointensity record from the Pacific Equator. Earth Planet. Sci. Lett. 374, 227–238.

Olson, P., Coe, R.S., Driscoll, P.E., Glatzmaier, G.A., Roberts, P.H., 2010. Geodynamo reversal frequency and heterogeneous core–mantle boundary heat flow. Phys. Earth Planet. Inter. 180, 66–79.

Pälike, H., Norris, R.D., Herrle, J.O., Wilson, P.A., Coxall, H.K., Lear, C.H., Shackleton, N.J., Tripati, A.K., Wade, B.S., 2006. The heartbeat of the Oligocene climate system. Science 314, 1894–1898.

Pälike, H., Lyle, M., Nishi, M., Raffi, I., Gamage, K., Klaus, A., The Expedition 320/321 Scientists, 2010. Proc. IODP, 320/321. Integrated Ocean Drilling Program Management International, Inc., Tokyo. http://dx.doi.org/10.2204/iodp.proc.320321.2010.

Pälike, H., et al., 2012. A Cenozoic record of the equatorial Pacific carbonate compensation depth. Nature 488, 609–614. http://dx.doi.org/10.1038/nature11360.

Pares, J.M., Lanci, L., 2004. A Middle Eocene–Early Eocene magnetic polarity stratigraphy in equatorial Pacific sediments. In: Channell, J.E.T., Kent, D.V., Lowrie, W., Meert, J.G. (Eds.), Timescales of the Paleomagnetic Field. Amer. Geophysical Union, Washington, DC, pp. 131–140.

Percival, D.B., Walden, A.T., 1993. Spectral Analysis for Physical Applications: Multi-Taper and Conventional Univariate Techniques. Cambridge University Press, Cambridge.

Schneider, D.A., 1995. Paleomagnetism of some Ocean Drilling Program Leg 138, sediments: Detailing Miocene stratigraphy. In: Pisias, N., Mayer, L.A., Janecek, T. et al. (Eds.), Proc. ODP, Sci. Results. Ocean Drilling Program, College Station, TX, pp. 59–72.

Shackleton, N.J., Crowhurst, S., Hagelberg, T., Pisias, N.G., Schneider, D.A., 1995. A new Late Neogene time scale: Application to Leg 138 sites. In: Pisias, N.G., Mayer, L.A., Janecek, T. et al. (Eds.), Proc. ODP, Sci. Results, Ocean Drilling Program, College Station, TX, 138, pp. 73–104.

Shipboard Scientific Party, Site 1090, 1999. In: Gersonde, R., Hodell, D.A., Blum, P. et al., (Eds.), Proc. ODP Init. Repts, 177, pp. 1–97 [CD ROM]. Available from Ocean Drilling Program, Texas A&M University, College Station, TX 77845–9547, USA.

Shipboard Scientific Party, Site 1218, 2002. In: Lyle, M., Wilson, P.A., Janecek, T.R. et al. (Eds.), Proc. ODP, Init. Repts., 199, pp. 1–125 [CD ROM]. Available from Ocean Drilling Program, Texas A&M University, College Station, TX 77845–9547, USA.

Tauxe, L., 1993. Sedimentary records of relative paleointensity of the geomagnetic field: theory and practice. Rev. Geophys. 31, 319–354.

Tauxe, L., Hartl, P., 1997. 11 million years of Oligocene geomagnetic field behavior. Geophys. J. Int. 128, 217–229.

Thomson, D.J., 1982. Spectrum estimation and harmonic analysis. Proc. IEEE 70, 1055–1096.

Westerhold, T., Röhl, U., Wilkens, R., Pälike, H., Lyle, M., Jones, T.D., Bown, P., Moore, T., Kamikuri, S., Acton, G., Ohneiser, C., Yamamoto, Y., Richter, C., Fitch, P., Scher, H., Liebrand, D., The Expedition 320/321 Scientists, 2012. Revised composite depth scales and integration of IODP Sites U1331–U1334 and ODP Sites 1218–1220. In: Pälike, H., Lyle, M., Nishi, H., Raffi, I., Gamage, K., Klaus, A., The Expedition 320/321 Scientists (Eds.), Proc. IODP, 320/321. Integrated Ocean Drilling Program Management International, Inc., Tokyo. http://dx.doi.org/10.2204/iodp.proc.320321.201.2012.

Xuan, C., Channell, J.E.T., 2009. UPmag: MATLAB software for viewing and processing u-channel or other pass-through paleomagnetic data. Geochem. Geophys. Geosyst. 10, Q10Y07. http://dx.doi.org/10.1029/2009GC002584.

Yamamoto, Y., Yamazaki, T., Acton, G.D., Richter, C., Guidry, E.P., Ohneiser, C., 2013. Paleomagnetic study of IODP Sites U1331 and U1332 in the Equatorial Pacific – extending relative geomagnetic paleointensity observations through the Oligocene and into the Eocene. Geophys. J. Int. http://www.dx.doi.org/10.1093/gji/ggt412.

Yamazaki, T., 2012. Paleoposition of the intertropical convergence zone in the eastern Pacific inferred from glacial–interglacial changes in terregenous and biogenic magnetic mineral fractions. Geology 40, 151–154.

Yamazaki, T., Yamamoto, Y., Acton, G., Guidry, E.P., Richter, C., 2013. Rock-magnetic artifacts on long-term relative paleointensity variations in sediments. Geochem. Geophys. Geosyst. 14 (1). http://dx.doi.org/10.1029/2012GC0004546.